

REPORT DOCUMENTATION PAGEForm Approved
OMB NO. 0704-0188

Public Reporting burden for this collection of information is estimated to average 1 hour per response, including the time for reviewing instructions, searching existing data sources, gathering and maintaining the data needed, and completing and reviewing the collection of information. Send comment regarding this burden estimates or any other aspect of this collection of information, including suggestions for reducing this burden, to Washington Headquarters Services, Directorate for information Operations and Reports, 1215 Jefferson Davis Highway, Suite 1204, Arlington, VA 22202-4302, and to the Office of Management and Budget, Paperwork Reduction Project (0704-0188,) Washington, DC 20503.

1. AGENCY USE ONLY (Leave Blank)	2. REPORT DATE -	3. REPORT TYPE AND DATES COVERED FINAL 01 Aug 96 - 31 Jul 98
4. TITLE AND SUBTITLE Si Based Nanostructure Growth Subsystem with Atomic Scale Control. Supersonic Molecular Beam Array Cell		5. FUNDING NUMBERS DAAH04-96-1-0364
6. AUTHOR(S) Kang L. Wang		
7. PERFORMING ORGANIZATION NAME(S) AND ADDRESS(ES) University of California - Los Angeles		8. PERFORMING ORGANIZATION REPORT NUMBER
9. SPONSORING / MONITORING AGENCY NAME(S) AND ADDRESS(ES) U. S. Army Research Office P.O. Box 12211 Research Triangle Park, NC 27709-2211		10. SPONSORING / MONITORING AGENCY REPORT NUMBER ARO 36240.1-RT-RIP
11. SUPPLEMENTARY NOTES The views, opinions and/or findings contained in this report are those of the author(s) and should not be construed as an official Department of the Army position, policy or decision, unless so designated by other documentation.		
12 a. DISTRIBUTION / AVAILABILITY STATEMENT Approved for public release; distribution unlimited.		12 b. DISTRIBUTION CODE
13. ABSTRACT (Maximum 200 words) The Following Equipment was Purchased: KSA 400 Computer System Si Molecular Beam Epitaxy System Compact Modular Plasma System This equipment was used to perform research in an effort to determine the mechanism of facet growth occurring in selective epitaxial growth and to produce Si based nanostructures using a supersonic molecular beam.		
14. SUBJECT TERMS		15. NUMBER OF PAGES
		16. PRICE CODE

20010227 142

UCLA

Final Report

I. Results from Grant DAAH04-96-1-0364

a. Overview

The grant had been used to purchase equipment and to support the researches including the PhD dissertation researches of two graduate students, in an effort to determine the mechanisms of facet growth occurring in selective epitaxial growth and accomplish Si-based nanostructures using a supersonic molecular beam. Publications from this grant are listed in the section of Publications.

The overall objective of this research program was to establish new instrumentation for being capable of better control of nano-structures via *in-situ* facet growth during selective epitaxial growth (SEG) using supersonic molecular beam array cell. There are several advantages to the use of supersonic molecular beams instead of conventional gas sources. The high kinetic energy of the molecules in a supersonic beam can allow them to overcome activation energy barriers of reactions with the existing surface species and thus to promote the growth process at low substrate temperature. The efficiency of incorporation of precursor species into the film can be increased nearly to unity if the kinetic energy of reactants exceeds the activation energy and steric restriction is overcome [6]. The molecules carry the energy necessary for the reactions and do not release it until they collide with the surface and the energy is turned into a highly localized "thermal spike". Thus, epitaxial growth can be achieved at very low substrate temperatures and atomic layer epitaxial (ALE) growth is also possible.

SEG growth is illustrated in Fig. 1, where a faceted structure narrows the (100) surface, which was used to realize the nanostructures and was also used as templates for subsequent heterogeneous nanostructure growth. The high molecular energy was tuned to overcome the activation energy barriers of the reactions and made it possible to achieve low temperature growth, which could significantly suppress the surface segregation and increase the thickness of the strained heterostructures. Nanoscale structures were realized by facet growth during *in-situ* selective epitaxial growth, which is a very promising technique for the application in nanometer quantum structures. In particular, we will address the mechanism of the *in-situ* nanometer growth, perform the nanostructures of Si and SiGe, and study the quantum characteristics of the nanostructures. The proposed research in SEG technology will be important for further advancement of microelectronics in the next decades.

The facet growth technique primarily relies on converging slow-growth planes and is dependent upon the interplay among substrate orientation, geometry, and growth conditions. Facet growth provides a means to shrink the Si (100) mesa beyond its original definition, since facets consume the mesa top as the epitaxial thickness increases. The precise control of this effect can lead to nanoscale structures at the top of the mesa (a template e.g., subsequent growth of quantum dots), thereby achieving lateral confinement. (Most previous efforts had focused on re-growth of AlGaAs/GaAs on predefined mesa stripes [1-4] but ours is a single and simpler process). In applications, Si-based nanostructures are especially important, as Si technology is the primary driver for microelectronics.

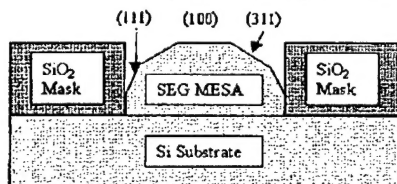


Fig. 1. Schematic diagram of the facet formation on a patterned substrate.

This research program focused on gas source molecular beam epitaxy (GSMBE) using Si₂H₆ and solid source Ge to fabricate the SEG structures. Others [5] have used chemical vapor deposition, CVD, (SiH₂Cl₂, GeH₄, H₂) to produce SEG structures. Our approach of combining gas and solid

sources offers several benefits. For example, the combination of GeH_4 and a gas-source silicon precursor results in non-linear growth rates and non-linear Ge incorporation rates as a function of the GeH_4 mole fraction as in CVD, while a solid source Ge and a gas source silicon precursor (Si_2H_6) provide linear growth rates and compositions. The lower pressure associated with GS-MBE allows growth to occur in the mass-transfer limited regime at lower temperatures (550 - 600 °C) than is associated with CVD growth [6,7], which typically operates in the surface reaction rate-limited regime [8]. In addition, the use of gas beams in lieu of CVD affords us selection of the beam energy by the use of supersonic jet sources. One apparent shortcoming associated with using a solid source here is that the growth is not strictly selective. We observe polycrystalline SiGe deposits on masked regions, although epitaxial material is selectively deposited on the exposed substrates. The polycrystalline deposits actually simplify the growth issue to some extent as loading effects [9] are greatly reduced. In our study, we utilized many different characterization techniques to monitor the structural integrity of Ge/Si SEG films. The primary sources of information included: 1) double and triple-axis x-ray diffraction measurements to ascertain the composition and stress state as well as to evaluate the overall crystalline quality; 2) atomic force microscopy (AFM); 3) transmission electron microscopy in both cross-section (XTEM) and plan-view to determine not only topology but also gain structural information, particularly in the case of SiGe SEG; and 4) Raman and low-temperature photoluminescence (PL) as a means to both corroborate other results and address confinement issues.

Our studies led to an understanding of the relationships among substrate orientation, geometric alignment, and growth kinetics. For example, we have investigated facet growth of Si on (100), (311), (111), and (110) substrates for both lines and squares. A mask, which was used to delineate such features, is shown in Fig. 2. These initial experiments help establish a basis for a minimization of total energy model, where volume energy is in direct competition with surface energy contributions which includes contributions of surface migration on each slow growth plane [10] [11].

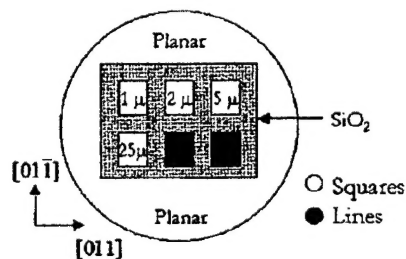


Fig. 2. A schematic of a processed 50 mm wafer and light micrographs of 1 μm , 2 μm , 5 μm , and 25 μm features. Each field contains a uniform patterned array, each having 50 % surface coverage. In this way, a single growth run can investigate SEG growth on 6 different fields and planar growth simultaneously. A mask, which has feature sizes below 0.1 μm was also used.

Examples of significant results are discussed below. As a result of our initial measurements of Si SEG on various orientations, the $\langle 110 \rangle$ feature alignment was identified to be the most efficient to reduce the (100) mesa. **One of the discoveries** was the observation of the ordering of Ge quantum dots along the convex surface of vicinal wafers and on selectively grown silicon mesas grown with supersonic molecular beam array cell, leading to the concept of preferential nucleation. **Another discovery** was the observation of the self-regulation in the formation of self-assembled Ge quantum dots, leading to the control of the nanostructures growth. This discovery simultaneously observed by us and by Kamins and Williams [12] led to the concept of self-registration of dot arrays. Our accomplishments of this research will impact the applications based on nanostructures.

In the following, we highlight our results into four main parts: (i) discussion of the new equipment, (ii) facet growth occurring within $\text{Si}_{1-x}\text{Ge}_x$ SEG ($x \leq 0.2$), and (iii) characterization of periodic three-dimensional structures, and (iv) growth of quantum dots and arrays.

b. Analysis of selected results

i. Equipment

The subsystem setup is illustrated in Fig. 3, showing the supersonic jet, monitoring equipment consisting of a pyrometric interferometer (PYRITTE), a RMEED, K-space KS300 system, UHV manipulator, 6" substrate heater and 6" substrate load-lock. More detail diagrams of the supersonic jet and PYRITTE are given in Figs. 4 and 5, respectively.

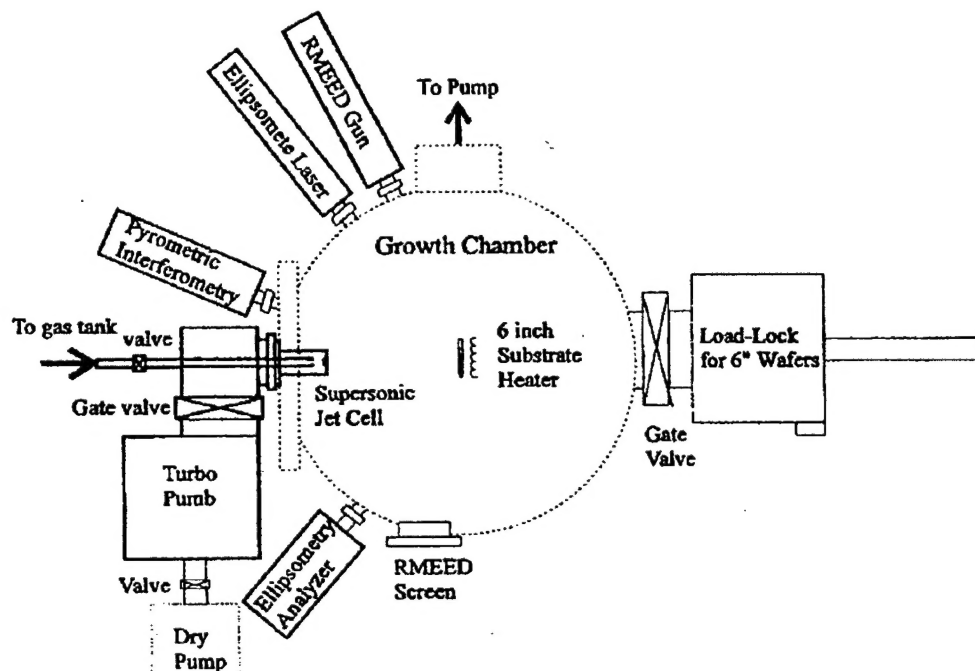


Fig.3 A 6"-GSMBE system with peripheral subsystems

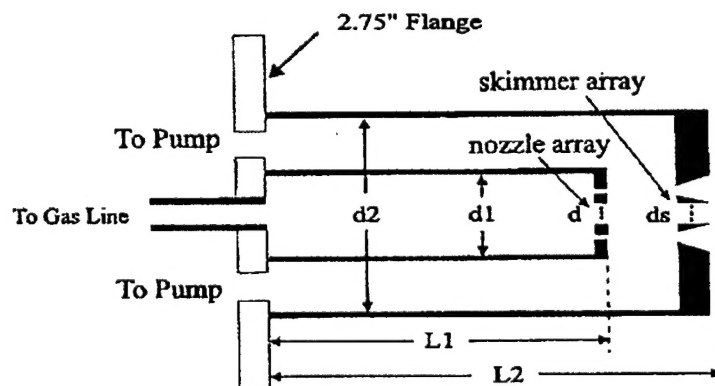


Fig. 4 A supersonic molecular beam array cell with a nozzle array and a skimmer.

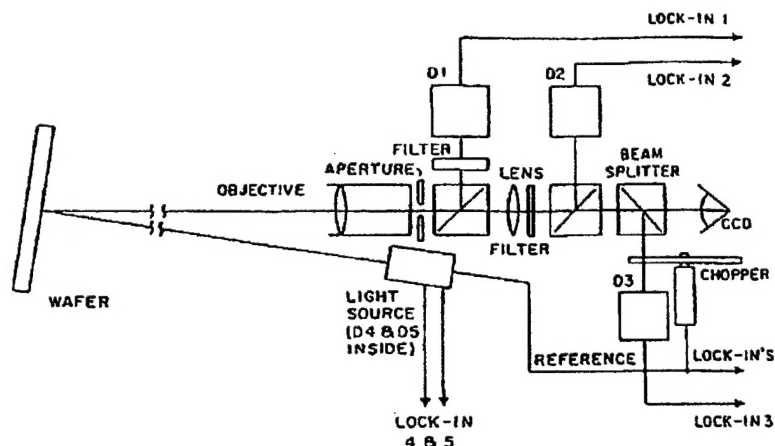


Fig. 5 Pyrometric interferometry measurement system

ii. Facet formations in SiGe SEG

In this research, we conducted a series of SEG experiments to better understand the dynamics of facet growth occurring in SiGe/Si heterostructures grown by gas source molecular beam epitaxy (GS MBE) with supersonic beam array. The pinhole of the beam array was 0.2 mm and the holes covered the whole area with the diameter of 2 inches. The typical stagnation pressure was 0.5 torr and the pressure in the growth chamber during growth was 1×10^{-5} torr. We used "wire" and "square" windows. Our goals included: a) exploring the differences in faceting in SiGe compared with Si, b) determining the role of the mask alignment on facet growth, and c) understanding the size dependence of facet growth such that it is feasible to achieve lateral confinement.

Each SEG experiment contains six different $4 \times 5 \text{ mm}^2$ fields of uniform rectangular geometry varying from 1-25 μm maintaining 50% surface coverage for each field (see Fig. 2). The opening features here were aligned parallel to the $\langle 110 \rangle$ directions. In addition to the SEG regions, the periphery of the substrate was left open for planar growth comparisons. Different SEG growth experiments were carried out as a function of a single variable, e.g. varying either the total epilayer thickness or composition. For all growth experiments, the epilayer thickness was chosen to be below the Matthews-Blakeslee critical thickness to avoid strain relaxation. X-ray diffraction and TEM results confirmed that the layers were pseudomorphic. A dark field XTEM micrograph of $\text{Si}_{0.9}\text{Ge}_{0.1}$ ($\epsilon = 3.9 \times 10^{-3}$) selective epilayer from a 5 μm lateral feature and 965 \AA in thickness is shown in Fig. 6, illustrating that the selective growth areas are defect-free. Both $\{311\}$ - and $\{111\}$ -type facets can be identified for this case while under the same growth conditions, the same lateral size, and thickness, Si SEG growth gave a single $\{311\}$ -type facet only. The facet growth does not seem to nucleate immediately at the heterointerface; the SiGe epilayer is partially in contact with the SiO_2 for approximately 50 \AA before the $\{111\}$ -type facet grows away from the boundary. The difference between Si and SiGe facet growth suggests that misfit strain or perhaps surface segregation plays an important role in facet formation. [12]

For SiGe alloy growth, either gaseous (GeH_4) or physical transport (evaporation) can provide the delivery of Ge to the substrate in GS-MBE. In terms of selectivity for SEG experiments, GeH_4 has the obvious advantage, but the process cannot be done at low temperature due to the thermal energy needed to facilitate the Ge-H decomposition. In our case, Ge evaporation is used, but in this case, selectivity is severely limited. A selective area diffraction pattern is shown in the inset of Fig. 6, which includes the selective epilayer and the SiO_2 mask regions. Debye-Scherrer rings for $\{111\}$ SiGe epilayer are observed

and are identified as originating from polycrystalline material on the SiO_2 masking layer. The grains are confined to the masking layer and do not seem to interfere with the selective growth process. In fact, the deposition of polycrystalline material seems to minimize loading-related effects. This was confirmed with double-axis x-ray diffraction measurements where no loading effect was observed for our lateral features ($\geq 1 \mu\text{m}$ for this mask). These XTEM results confirm RHEED observations taken during crystal growth, where Debye-Scherrer rings were superimposed on a (2×1) spot pattern immediately after initiating SiGe growth.

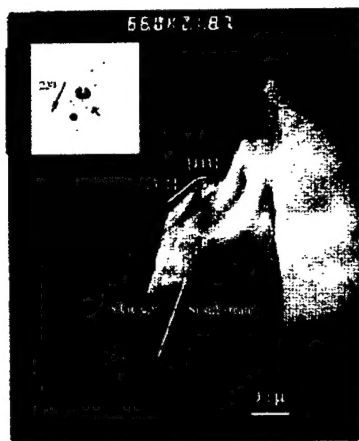


Fig. 6 A [220] dark field XTEM micrograph of selective $5 \mu\text{m}$ lateral feature. A double facet is observed, identified as the $\{311\}$ - and $\{111\}$ -type. The inset is the inverted selective area diffraction pattern taken over the selective epi and masking oxide layers. The marker points to evidence of $\{111\}$ Debye-Scherrer rings, albeit only a few grains are contributing.

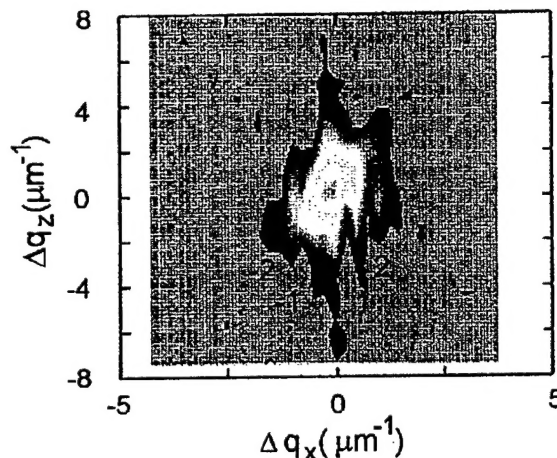


Fig. 7 A (400) reciprocal space map about the Si Bragg peak of an array of $0.5 \mu\text{m}$ lateral SEG features. The in-plane periodicity gives rise to superlattice peaks in Δq_x . Here, the ± 2 orders are visible

We also observe a correlation between the lateral window size and contact length, where the trend follows a square-root dependence, suggesting kinetic behavior. In some cases, we observe cusp formation and the cusp forms as a result of different migration lengths on crystallographic surfaces; here, the presence of a cusp indicates that surface diffusion on the facet planes is faster than on the (100) surface [13]. Facet growth is a dynamic growth process of facet competition. Adatoms on the facets migrate up the diagonal and build a cusp, where the supersaturation is higher. From these results, geometry not only influences the degree of the cusp, but also determines the temporal evolution of growing facets since facet growth seems to nucleate at much earlier stages for smaller geometries. This seems reasonable. As the selective area begins to approach the diffusion length, adatoms will require shorter distances to migrate before reaching the lowest energy site. A size effect is expected, and these results are in qualitative agreement with a minimization of total energy (volume and surface) model [14].

iii. Triple-Axis x-ray diffraction of corrugated surfaces

Structures with an in-plane modulation - including patterned SEG or grating structures - can be analyzed by triple axis x-ray diffraction measurements. Satellite peaks, which correspond to the in-plane modulation, are observed in reciprocal space maps. Others have investigated this phenomenon for simple geometric profiles, but the technique is actually much more powerful than has been previously shown and can be applied to any geometric profile for which a Fourier transform can be generated. Both the geometry of the structures and lattice strains can be quantified through the analysis of these satellite peaks [15-17]. The presence of strain in the periodic features introduces a shift in the diffraction envelope from

these features; this displacement can be observed using asymmetric reflection geometry, and can be quantified and converted to a strain matrix [18,19]. We have extended the application of reciprocal space mapping of in-plane modulated structures to study processing issues associated with nanostructured materials.

First, we developed a kinematical diffraction simulation program to quantify the in-plane geometric profile. The initial application of this model involved changes in the geometric profile of a grating etched in a substrate during high temperature annealing [20]. These models have been refined in our study of the SiGe SEG structures to support the TEM measurements. Second, we have modeled the change in the strain distribution in an in-plane modulated structure, which was buried by a subsequent epitaxial overgrowth layer. In this case, we used dynamical diffraction models to extract the strain distribution along the growth direction. This was the first published report of determining the strain gradient of an in-plane modulated structure by using dynamical theory. A program based on the combination of the kinematical theory for the shape factor and dynamical theory for the strain distribution has been developed to allow us to use reciprocal space mapping to extract information about the SEG growth.

An early example of the use of reciprocal space mapping to study SEG is shown in Fig. 7. In this case, a Si buffer was selectively grown over a 0.5 μm feature. The in-plane periodic array of the three-dimensional silicon structures gives rise to satellite peaks along the Δq_x (in-plane) direction. The satellite peaks are centered slightly below the main Si Bragg reflection as shown by the dashed line. A slight strain in the Si buffer layer stems from the difference in the thermal expansion between the oxide mask and the Si buffer. This strain is on the order of $8 \cdot 10^{-5}$ and is modeled using our dynamical diffraction program. Because the strain is so small for this example, modeling the distribution as either a linear strain gradient or as a two-layer structure with the lower layer strained and the top layer relaxed gives about the same fit to the data. Modeling strain for the SiGe structures is much less ambiguous. We anticipate that reciprocal space mapping will continue to be an important non-destructive measurement technique for the SEG structures.

iv. Growth of Ge quantum dots and dot arrays

RHEED (Reflection high electron energy diffraction) is a well-established *in-situ* monitoring tool for conventional epitaxial growth. For studying nanostructures on patterned substrates and subsequently deposited self-organized dots, a lower electron energy beam (referred to reflection medium energy electron diffraction (RMEED)) was used to study the facet growth and nanostructure formation, which has a similar working principle with RHEED. The use of a lower electron beam energy enables us to increase the resolution in the RMEED patterns and thus to improve the sensitivity in determining the strain of nanostructures. The evolution of typical Ge nanostructure growth on Si substrates is the formation of a two-dimensional monolayer at the beginning and then the start of three-dimensional growth or island formation, which is referred as to Stranski-Krastanov growth mode. Fig. 8 depicts our previous results of the typical RHEED patterns from Si(100) surface, indicating streaky (2×1) structure, which is indicative of an atomically smooth surface. After the formation of self-organized Ge dots, the half orders of the pattern become blurred gradually and chevrons appear, which represent the facets of the dots. With the KSA400 RHEED analysis assembly, which consists of a CCD recorder and a powerful software, we are able to *in-situ* analyze the RHEED patterns during growth transitions and to determine the surface strain by studying the change of the lattice constants.

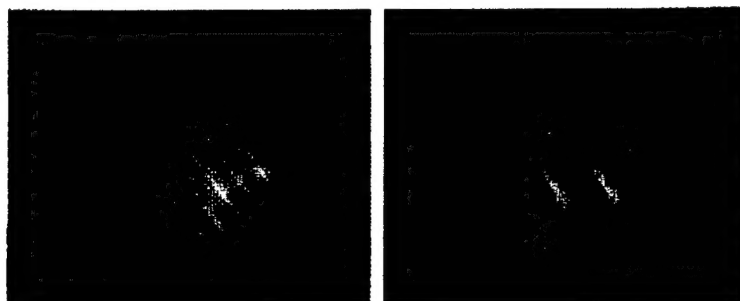


Fig. 8 MHEED patterns taken (left) from a clean Si(100) surface after desorption of native oxide layer, and (right) after growth of a Si buffer layer and 10ML Ge on the substrate.

The formation of coherent, strained three-dimensional (3D) Ge dots on planar substrates has been received much attention, in the pursuit of exploiting the electronic quantum confinement as a result of inherent low-dimensions. However, dot distribution is typically random and there is a wide size distribution. In order to understand and control the growth of quantum sized nanostructures on the mesas we have performed systematic experimental studies of quantum dot deposition on the Si SEG mesas as well as tilted Si substrates. It was found that it is possible to grow high quality uniform sized Ge quantum dots on the planar Si substrates. Fig. 9 shows the AFM image of uniform Ge quantum dots on planar Si (001). [22] It can be seen that the Ge dots have a very good and uniform size distribution. One of the most critical issues in the application of quantum dots is the exact placement of dot arrays on the designated sites in addition the control of size uniformity. The possibility of controlling the dot location on the Si facets has also been demonstrated in our previous research on surface miscut Si substrate [23], which has atomic height steps. In addition to similar uniformity of dot size distribution, we have also observed the self-alignment of the Ge dots on the convex upper-edges of the undulated surface, suggesting that it is possible to have good control over both the dot size uniformity and location. This preferred placement may arise from the strain minimization of the convex surface. A detailed high-resolution TEM analysis of strain appears to support this supposition [23]. This is very promising in terms of its applications in optoelectronic devices.

To further understand the growth of Ge quantum structures, we have also demonstrated the possibility of forming Ge quantum wires on miscut Si substrate. As shown in Fig. 10, high quality Ge quantum wire arrays are formed on the upper-edges of the miscut surface atomic steps. We believe that the wires are formed by initially closely packing self-aligned Ge dots along the upper-edges of the steps [24]. Our work demonstrates the possibility of controlling both the size uniformity and location of the nanostructures by direct GSMBE growth. This idea leads to the study of quantum dots and wires on pre-designed SEG mesas with good size and location control.

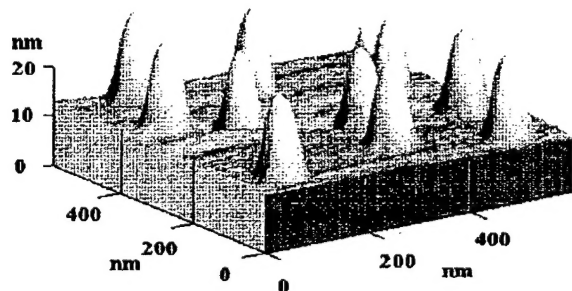


Fig. 9 An atomic force micrograph of a Si SEG template used for the deposition of Ge quantum dots. This example demonstrates the very good control of the dot size uniformity.

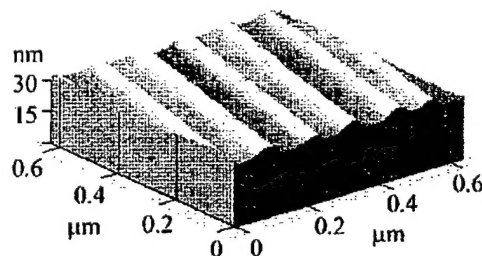


Fig. 10 AFM image of high quality Ge quantum wires grown on miscut Si substrate

Selective epitaxial growth (SEG) is an important growth technique due to its capability of fabricating devices on patterned samples without breaking the growth. During SEG process on an $\langle 110 \rangle$ -oriented patterns, $\{113\}$ facets are formed at the earlier stage of growth, leading to the shrinkage of the top surface region and finally the full reduction and formation of one-dimensional ridges. Therefore, we controlled the formation of the SEG mesas to achieve one-dimensional ridges on stripe Si patterns in attempt to form an ordered dot array. Fig. 11 a and b present respectively two- and three-dimensional AFM images of the self-assembled Ge dots on the $\langle 110 \rangle$ -oriented Si stripe mesas, formed in the exposed Si stripe windows. Perfectly aligned and regularly spaced one-dimensional array of the Ge dots was formed on the ridge of the Si stripe mesa. Similar result was reported by other groups [25,26]. The perfect alignment of the dots along the Si stripe mesas is attributed to self-regulation mechanism driven by the minimization of the total energy, and also assisted by the formation of the ridges [27]. The tendency of Ge quantum dots to form on the ridge (or near the edge of a lattice step or the intersection of facet planes) is a result of stress-driven kinetics. The edges are compliant, i.e., are most easily deformed by the dots growing on the facets. The dimensions of the Ge dots are about 80 nm wide and 20 nm high, and the period of Ge dots is about 110 nm. Moreover, the aligned Ge dots showed *mono*-modal morphology and size distribution on the ridges, which is very interesting as *bi*-(even *multi*-) modal distribution of self-assembled Ge dots is normally observed on planar Si (001) substrates. The *mono*-modal distribution is believed to be associated with the cooperative arrangement on the 1D ridges. The formation of the cooperative arrangement with *mono*-modal distribution provides a path to realize uniform dots as well as the control of the spatial arrangement.

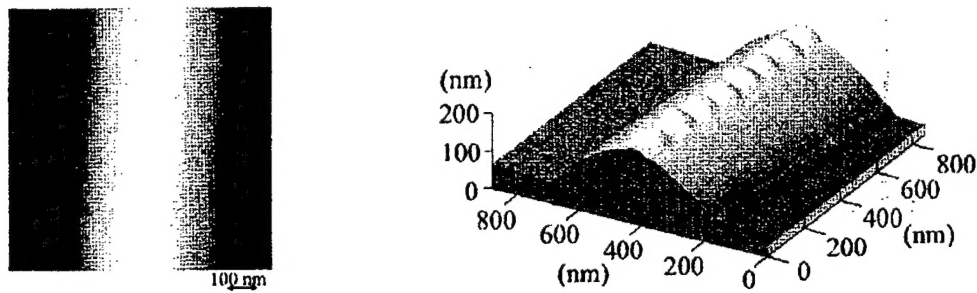


Fig. 11 (a) 2D and (b) 3D AFM images of self-assembled Ge dots on $\langle 110 \rangle$ -oriented Si stripe mesa with a base width of 0.55 μm . One-dimensional cooperative arrangement of Ge dots is formed on the ridge of the Si mesa after the deposition of 10 ML Ge at a growth temperature of 600°C.

Vertical and lateral ordering in quantum dot Ge/Si structures indicates that the strain distribution in the underlying material influences the deposition location of the dots [28-33]. In the case of a multi-layer of quantum dots / wetting layers and barrier layers of the appropriate thickness, the quantum dot structures tend to align over previously formed dots. The strain from the underlying 3-D dot transfers through the barrier layer and provides a favorable nucleation site, leading to the vertical alignment of Ge dots as shown in Fig. 12 a and b. One can see that the true vertical alignment occurs after the third layers in Fig. 12a and the alignment orientation slightly deviates from the $[100]$ direction. The Ge dots from the third layer show the good vertical correlation and uniformity in the multiplayer structure, which is different with the previously reported results, i.e. the dots in the upper layers were larger than those in the lower layers. This result demonstrates the possibility of forming 3D structured uniform dots with multiplayer structure.

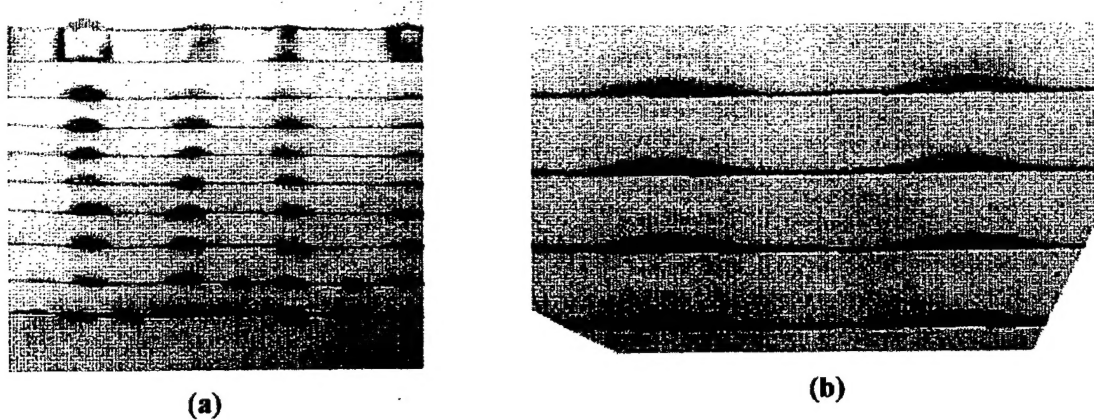


Fig. 12 (a) Dark-field cross section TEM image taken from the sample with ten layers of Ge quantum dots, showing the vertical alignment. It is also noted that there are some changes of the alignment between the first three layers. (b) Bright-field cross section TEM image of the same sample, showing the good vertical alignment and uniform dots in the upper layers. The thicknesses of Ge layers and Si spacer layers are 1.6 nm and 40 nm, respectively.

The properties of quantum dots have been gained a great interest for applications. [34-39] Fig. 13 presents the photoluminescence spectrum taken from a sample with 10-layer Ge dots at the temperature of 8 K, showing the contribution from Ge wetting layers and Ge quantum dots. The double peak at about 0.8 eV is the contribution of Ge quantum dots. The photoluminescence from Ge dots at about 0.8 eV was observed at room temperature as shown in Fig. 14, albeit peaks from Ge wetting layers and Si disappeared. This is due to the quantum confinement effect, therefore, the excitons in dots quench at higher temperature at about 100 K compared with 25 K for Ge wetting layers. The merit of photoluminescence from Ge dots at room temperature will perhaps impact the optoelectronic applications.

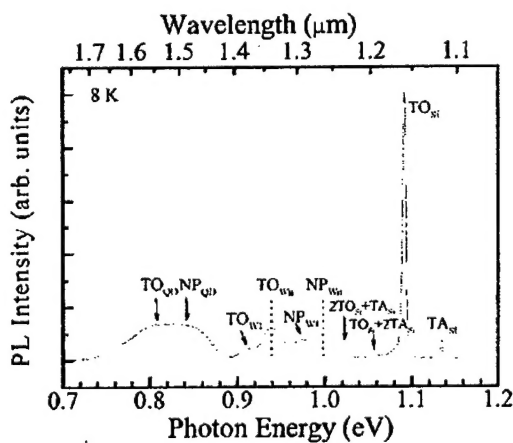


Fig. 13 Photoluminescence spectrum taken at 8 K from a sample with 10 stacked layers of self-assembled Ge dots on planar Si (001) substrates. The peaks at about 0.8 eV are related to the Ge quantum dots. The separation between the TO_{QD} and NP_{QD} peaks is 40 meV.

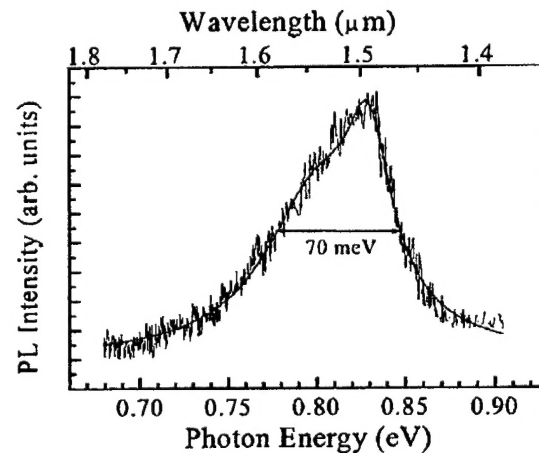


Fig. 14 Photoluminescence spectrum taken at room temperature, only showing the peaks at about 0.8 eV or 1.55 μm attributed to Ge quantum dots. The full width at half maximum of the double peak is about 70 meV.

Strain is believed to be an important parameter for the subsequent placement of quantum dots. In fact, we observed the non-uniform strain distribution on SEG mesas with micro-Raman measurements.

It was found that there was a tensile strain at the edges of Si SEG mesas. Therefore, Ge dots were preferentially located along the edges as shown in Fig. 15 and 16. This preferential nucleation enables to control the dot positioning. As the lateral dimensions shrink, it is expected that the additional free surfaces [facets and the original (100)] will offer some strain relief, in contrast with a two-dimensional film [40-42].

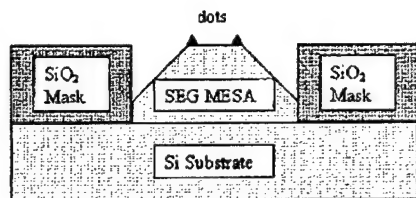


Fig. 15 Schematics of an example of self-regulated nanostructure formation on top of a SEG template.

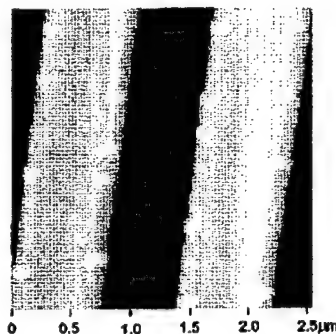


Fig. 16 An atomic force microscopic image of a Si SEG template used for the deposition of Ge quantum dots.

Further studies on the control of Ge dot positioning have been conducted and the AFM results are shown in Figs. 17 and 18. Four pyramidal Ge dots are located at the corners of the pre-grown Si mesas as shown in Fig. 17. Several different configurations of the positioning have also been observed with the variation of the Ge thickness deposited. One dot on each Si mesa has been obtained at the growth temperature of 700°C shown in Fig. 18. Controlled growth on pre-grown Si mesas allows us to realize the true control of Ge quantum dot positioning, even for a single dot. Given the results of the vertical strain-induced ordering and the success of forming localized quantum dots by a homoepitaxial template, the possibility is that the strain distribution present in a 3-D feature such as a strained layer SiGe SEG be used to further control and to allow for more precise placement of quantum dot arrays.

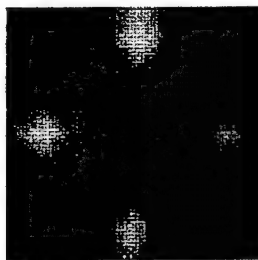
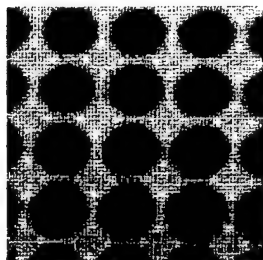


Fig. 14 Two-dimensional AFM images of 2D arrangement of Ge dots with 0.8 nm Ge at growth temperature of 600°C, (left) Four Ge dots are arranged on each unit of Si mesas, sacn area: $4 \times 4 \mu\text{m}^2$; (right) Magnified view of a unit cell in (a).

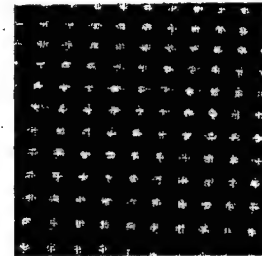
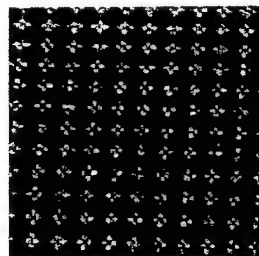


Fig. 15 Two-dimensional AFM images of 2D arrangement of Ge dots. (left) Growth temperature is 650°C, four Ge dots are arranged on each unit of Si mesas; (right) Growth temperature is 700°C, only one Ge dot is arranged on each unit of Si mesas. Both the sacn areas are $4 \times 4 \mu\text{m}^2$.

Significance and impact of this research:

This research has yielded significant results, which impact the understanding of the growth mechanisms of nanostructures based on the faceted growth with supersonic molecular beam array cell, and demonstrate the control of self-assembled dot array growth in size and placement with the SEG mesas. The controlled growth is critical for applications of nanometer scale arrays in electronic and optoelectronic devices, such as nearest neighbor interaction computational systems for the next Millenium beyond the limitation of today's CMOS. The research provides a potential route in the advanced Si-based microelectronics, leading to the new era of nanoelectronics.

II. Publications

- P1. S. Li, Q. Xiang, D. Wang, K. L. Wang, "Investigation of facet formation and competition in MBE growth," *J. Cryst. Growth* **164** (1996): 235-40.
- P2. Q. Xiang, S. Li; D. Wang; K. L. Wang, J. G. Couillard, and H. G. Craighead, "Interfacet mass transport and facet evolution in selective epitaxial growth of Si by gas source molecular beam epitaxy," *J. Vac. Sci. Technol. B* **14** (3): 2381 (1996).
- P3. D. Wang, S. Thomas, and K. L. Wang, "Nanometer Scale Patterning and Pattern Transfer on Amorphous Si, Crystalline Si, and SiO₂ Surfaces Using Self-Assembled Monolayers," *Applied Physics Letters*, **69**, 1593-1595, (1996).
- P4. Q. Xiang, S. Li, D. Wang, K. Sakamoto, K. L. Wang, G. U'Ren, and M. Goorsky, "Sidewall Faceting and Inter-Facet Mass Transport in Selectively Grown Epitaxial Layers on SiO₂-Masked Si(110) Substrates," *Journal of Crystal Growth*, **175/176**, 469-473, (1997).
- P5. M. A. Chu, M. O. Tanner, F. Huang, K. L. Wang, G. G. Chu, and M. S. Goorsky, "Photoluminescence and X-ray Characterization of Relaxed Si_{1-x}Ge_x Alloys Grown on Silicon on Insulator (SOI) and Implanted SOI Substrates," *Journal of Crystal Growth*, **175/176**, 1277-1283, (1997).
- P6. K. L. Wang and D. Wang, "Facet Formation in Submicron Selective Growth of Si/SiGe," *Material Research Society*, 241-251, 1997.
- P7. A. G. U. Perera, W. Z. Shen, W. C. Mallard, M. O. Tanner, and K. L. Wang, "Far-Infrared Free-Hole Absorption in Epitaxial Silicon Films for Homojunction Detectors," *Applied Physics Letters*, **70**, 515-517, (1997).
- P8. Y. S. Tang, S. Cai, G. Jin, J. Duan, K. L. Wang, H. M. Soye, and B. S. Dunn, "SiGe Quantum Dots Prepared on an Ordered Mesoporous Silica Coated Si Substrate," *Applied Physics Letters*, **71**, 2448-2450, (1997).
- P9. Y. S. Tang, S. Cai, D. Wang, G. Jin, J. Duan, K. L. Wang, H. M. Soye, and B. S. Dunn, "Control of Sizes and Optical Emission of SiGe Quantum Dots Prepared on Ordered Mesoporous Silica Coated Si Wafer," *Materials Research Society Proceedings*, 1997.
- P10. F.Y.Huang, Y.S.Tang, J.Duan & K.L.Wang, "Visible light emission from dry etched Si-SiGe quantum dots," *Electron. Lett.* **33**, 1736-1737 (1997)
- P11. Y.S.Tang, G.L.Jin & K.L.Wang, "Direct MBE Growth of Ge Dots on Ordered Meso-porous Glass Coated Si Substrate," 7th Int. Conf. on Si-MBE, Banff, Canada, June 1997; *Thin Solid Films*, **321**, 76-80 (1998).
- P12. X. Zhu, X. Zheng, M. Pak, Mo.O. Tanner, and K.L. Wang, "A Si bistable diode utilizing interband tunneling junctions," *Appl. Phys. Lett.* **71**, 2190-2192, (1997).
- P13. K. Schmalz, I.N. Yassievich, K.L. Wang and S.G. Thomas, "Localized-state band induced by B δ -doping in Si/Si_{1-x}Ge_x/Si quantum wells," *Physical Review B* **57**, 6579-6583, (1998).
- P14. J.L. Liu, S.J. Cai, G.L. Jin, and K.L. Wang, "Wirelike Growth of Si on an Au/Si(111) Substrate by Gas Source Molecular Beam Epitaxy," *Electrochemical and Solid-State Letters*, **1**, 188-190 (1998).
- P15. K. Sakamoto, H. Matsuhata, M. Tanner, D. Wang, K. L. Wang. "Alignment of Ge three-dimensional islands on faceted Si(001) surfaces," *Thin Solid Films* **321**, 55-59(1998).
- P16. G. D. U'Ren, K. M. Matney, M. S. Goorsky, M. Wormington, E. M. Koontz, M. H. Lim, V. V. Wong, G. S. Petrich, L. A. Kolodziejski, and Henry I. Smith. "Analysis of Lattice Distortions in High Quality InGaAsP Epitaxial Overgrowth of Rectangular-Patterned InP Gratings." *J. Vac. Sci. Technol. B* **16** (3) 1381-1384 (1998).
- P17. G. D. U'Ren, M. S. Goorsky, E. M. Koontz, G. S. Petrich, L. A. Kolodziejski, M. H. Lim, V. V. Wong, Henry I. Smith, K. M. Matney, and M. Wormington. "Triple Axis Diffraction Studies of InP Grating Structures." *Adv. X-ray Anal.* **41** (1998).
- P18. E.M. Koontz, M.H. Lim, V.V. Wong, G.S. Petrich, L.A. Kolodziejski, Henry I. Smith, K.M. Matney, G. D. U'Ren, and M.S. Goorsky. "Preservation of Rectangular-Patterned InP Gratings Overgrown by Gas Source Molecular Beam Epitaxy." *Appl. Phys. Lett.* **71** (1997) 1400-1402.

- P19. U'Ren, G.D.; Goorsky, M.S.; Koontz, E.M.; Lim, M.H.; Petrich, G.S.; Kolodziejski, L.A.; Wong, V.V.; Smith, H.I.; Matney, K.M.; Wormington, M. *Analysis of lattice distortions in high-quality InGaAsP epitaxial overgrowth of rectangular-patterned InP gratings*. J. Vac. Sci. Techn. B 16, (1998), p.1381-4.
- P20. E. M. Koontz, G. D. U'Ren, M. H. Lim, L. A. Kolodziejski, M. S. Goorsky, G. S. Petrich, and Henry I. Smith. "Overgrowth of (In,Ga)(As,P) on Rectangular-Patterned Surfaces Using Gas-Source Molecular Beam Epitaxy." J. Cryst. Growth 198-199, (1999), p.1104-10.
- P21. J.L.Liu, W.G. Wu, A. Balandin, G.L. Jin, K.L. Wang, *Intersubband absorption in boron-doped multiple Ge quantum dot*, Applied Physics Letters, 74, 185 (1999).
- P22. J.L.Liu, Y.S.Tang, and K.L.Wang, T.Radetic and R. Gronskey, *Raman scattering from a self-organized Ge dot superlattice*, Applied Physics Letters, 74, 1863 (1999).
- P23. G. Jin, Y. S. Tang, J. L. Liu, and K. L. Wang, "Growth and optical properties of self-organized Ge quantum wires on Si (111) substrates", Applied Physics Letters, 74, 2471 (1999).
- P24. Liu, J.L.; Wu, W.G.; Balandin, A.; Jin, G.; Luo, Y.H.; Thomas, S.G.; Lu, Y.; Wang, K.L. *Observation of inter-sub-level transitions in modulation-doped Ge quantum dot*. Applied Physics Letters, 75, AIP, 20 (1999), p.1745-7.
- P25. G. Jin, J.L. Liu, S.G. Thomas, Y.H. Luo, K.L. Wang, Nguyen, B.Y. *Controlled arrangement of self-organized Ge islands on patterned Si (001) substrates*. Applied Physics Letters, 75, (1999), p.2752-4.
- P26. Wen-Gang Wu; Jian-Lin Liu; Yin-Sheng Tang; Wang, K.L. *Infrared spectroscopy of intraband transitions in Ge/Si quantum dot superlattices* Superlatt. Microstruct., 26, (1999), p.219-27.
- P27. G. Jin, Y. S. Tang, J. L. Liu, and K. L. Wang, "Self-organized Ge quantum wires on Si (111) substrates", J. Vac. Sci. Technol. B. 17, (1999), p.1406-1409.
- P28. J.L.Liu, W.G.Wu, Y.S.Tang, and K.L.Wang, T.Radetic and R. Groosky, *Raman scattering and infrared absorption in multiple boron-doped Ge dots*, submitted to J. Vac. Sci. Technol. B (10/98).
- P29. U'Ren, G.D.; Goorsky, M.S.; Wang, K.L. *Influence of misfit strain on {311} facet development in selective epitaxial growth of Si/sub 1-x/Ge/sub x/Si(100) grown by gas-source molecular beam epitaxy*, Thin Solid Films, 365, (no.1), (2000), p.147-50.
- P30. J.L. Liu, G. Jin, Y.S. Tang, Y.H. Luo, K.L. Wang, D.P. Yu, *Optical and acoustic phonon modes in self-organized Ge quantum dot superlattices*. Applied Physics Letters, 76, (2000), p.586-8.
- P31. J.L. Liu, G. Jin, Y.S. Tang, Y.H. Luo, Y. Lu, K.L. Wang, D.P. Yu, *Study of phonons in self-organized multiple Ge quantum dot*. J. Electr. Mat., 29, (2000), p.554-6.
- P32. G. Jin, J.L. Liu, Y.H. Luo, K.L. Wang, *Control of the arrangement of self-organized Ge dots on patterned Si(001) substrates*. Thin Solid Films, 369, (2000), p.49-54.
- P33. G. Jin, J.L. Liu, S.G. Thomas, Y.H. Luo, K.L. Wang, Nguyen, B.Y. *Perfect alignment of self-organized Ge islands on pre-grown Si stripe mesa*, Applied Physics A 70, (2000), p.551-4.
- P34. G. Jin, J. L. Liu, and K. L. Wang, *Regimented placement of self-assembled Ge dots on selectively grown Si mesas*, Applied Physics Letters, 76, (2000), p.3591-3.

III. Bibliography

1. Dilger, M. et al., Transmission electron microscopy studies of GaAs/AlGaAs heterostructures regrown on patterned substrates, Semicond. Sci. Technol. 1994, 9: p2258-2262.
2. Madhukar, A. Growth of semiconductor heterostructures on patterned substrate: Defect reduction and nanostructures, Thin Solid Films, 1993, 231: p.8-42.
3. Kasia, J. et al., Structure and optical characterizations of single three dimensionally confined GaAs/AlAs structures grown on patterned GaAs (001) substrates, J. Vac. Sci. Technol. B, 1997, 15: p.862-69.
4. Koshiba, S., et al., Formation of GaAs ridge quantum wire structures by MBE on patterned substrates, Appl. Phys. Lett., 1994, 64: p.363-5.
5. Vescan, L., et al., *Lateral confinement by low pressure chemical vapor deposition-based selective epitaxial growth of Si_{1-x}Ge_x/Si nanostructures*. J. Appl. Phys., 1997, 81(10): p. 6709-15.
6. Vescan, L., et al., *Si/SiGe dots grown by selective epitaxy*. Semicon. Sci. Tech., 1994, 9(1994): p. 387-391.
7. Yang, Y.N. and E.D. Williams, *The role of carbon in the faceting of Si surfaces on the (111) to (001) azimuth*. J. Vac. Sci. Technol. A, 1990, 8(3): p. 2481-8.

8. Q. Xiang, S. Li; D. Wang; K. L. Wang, J. G. Couillard, and H. G. Craighead, "Interfacet mass transport and facet evolution in selective epitaxial growth of Si by gas source molecular beam epitaxy," J. Vac. Sci. Technol. B **14** (3): 2381 (1996); S. Li, Q. Xiang, D. Wang, K. L. Wang, "Investigation of facet formation and competition in MBE growth," J. Cryst. Growth **164** (1996): 235-40.
9. Ishitani, A., N. Endo, and H. Tsuya, *Local Loading effect in Selective Si epitaxy*. Jpn. J. Appl. Phys., 1982. **23**(6): p. L391-L393.
10. Garnier, J.G.E., et al., *Influence of Temperature on the Crystal Habit of Silicon in the Si-H-Cl CVD system*. J. Cryst. Growth, 1989. **96**(1989): p. 821-831.
11. Li, S., et al., *Investigation of facet formation and competition in MBE growth*. J. Cryst. Growth, 1996. **164**(1996): p. 235-240.
12. U'Ren, G.D.; Goorsky, M.S.; Wang, K.L. *Influence of misfit strain on {311} facet development in selective epitaxial growth of Si/sub 1-x/Ge/sub x/Si(100) grown by gas-source molecular beam epitaxy*, Thin Solid Films, **365**, (no.1), (2000), p.147-50.
13. Haider, N., M. Wilby, and D. Vvedensky, *Growth kinetics on non-planar substrates*. J. Cryst. Growth, 1993. **127**(1993): p. 992-926.
14. Aoyama, T., et al., *Facet formation mechanism of Si selective epitaxial layer by Si ultrahigh vacuum chemical vapor deposition*. J. Cryst. Growth, 1994. **136**(1994): p. 349-354.
15. Shen, Q., et al., *X-ray diffraction from a coherently illuminated Si (001) grating surface*. Phys. Rev. B, 1993. **48**(24): p. 17967-71.
16. Macrander, A.T. and S.E.G. Slusky, *X-ray diffraction from corrugated crystalline surfaces and interfaces*. Appl. Phys. Lett., 1990. **56**(5): p. 443-5.
17. Sluis, P.v.d., *High-resolution x-ray diffraction of periodic surface gratings*. Appl. Phys. Lett., 1993. **62**(24): p. 3186-8.
18. Holy, V., et al., *Elastic strains in GaAs/AlAs quantum dots studied by high-resolution x-ray diffraction*. Phys. Rev. B, 1995. **52**(11): p. 8348-57.
19. Shen, Q. and S. Kycia, *Determination of interfacial strain distribution in quantum-wires structures by synchrotron x-ray scattering*. Phys. Rev. B, 1997. **55**(23): p. 15791-97.
20. Koontz, E.M., et al., *Preservation of Rectangular-Patterned InP Gratings by Gas-Source Molecular Beam Epitaxy*. Appl. Phys. Lett., 1997. **71**(1997): p. 1400-1402.
21. U'Ren, G.D., et al., *Analysis of lattice distortions in high-quality InGaAsP epitaxial overgrowth of rectangular-patterned gratings*. J. Vac. Sci. Technol. B, 1998. **16**(3): p. 1381-4.
22. G. Jin, J.L. Liu, Y.H. Luo, K.L. Wang, Thin Solid Films, (in press)
23. Sakamoto, K., et al. *Alignment of Ge three-dimensional islands on faceted Si (001) surfaces*. in *7th International Symposium on Si Molecular Beam Epitaxy*. 1997. Banff: Thin Solid Films.
24. G. Jin, Y. S. Tang, J. L. Liu, and K. L. Wang, "Self-organized Ge quantum wires on Si (111) substrates", J. Vac. Sci. Technol. B. **17**, (1999), p.1406-1409.
25. Kamins, T.I. and R.S. Williams, *Lithographic positioning of self-assembled Ge islands on Si (001)*. Appl. Phys. Lett., 1997. **71**(9): p. 1201-3.
26. Zhang, R., et al., *Selective formation and alignment of InAs quantum dots over mesa stripes along the [011] and [001] directions on GaAs (100)*. Appl. Phys. Lett., 1998. **73**(4): p. 505-7.
27. G. Jin, J.L. Liu, S.G. Thomas, Y.H. Luo, K.L. Wang, Nguyen, B.Y. *Controlled arrangement of self-organized Ge islands on patterned Si (001) substrates*. Applied Physics Letters, **75**, (1999), p.2752-4.
28. Tersoff, J., C. Teichert, and M.G. Lagally, *Self-Organization in Growth of Quantum Dot Superlattices*. Phys. Rev. Lett., 1996. **76**(10): p. 1675-78.
29. Mateeva, E., et al., *Mechanism of organization of three-dimensional islands in SiGe/Si multilayers*. Appl. Phys. Lett., 1997. **71**(22): p. 3233-5.
30. Feng Liu; Lagally, M.G. *Strain-induced self-organization of steps and islands in SiGe/Si multilayer films*. Metallurgical and Materials Transactions A **29A**, (1998) p.2111-19.
31. Le Thanh, V.; Yam, V.; Boucaud, P.; Fortuna, F.; Ulysse, C.; Bouchier, D.; Vervoort, L.; Lourtioz, J.-M. *Vertically self-organized Ge/Si(001) quantum dots in multilayer structures*. Physical Review **B 60**, (1999) p.5851-7.
32. Holy, V.; Stangl, J.; Zerlauth, S.; Bauer, G.; Darowski, N.; Lubbert, D.; Pietsch, U. *Lateral arrangement of self-assembled quantum dots in an SiGe/Si superlattice*. J. Physics D **32**, (1999), p.A234-8.

33. Schmidt, O.G.; Eberl, K. *Multiple layers of self-assembled Ge/Si islands: Photoluminescence, strain fields, material interdiffusion, and island formation*. Physical Review B **61**, (2000) p.13721-9.
34. Tang, Y.S., et al., *Optical properties of dry etched Si/SiGe heterostructure wires*. Jpn. J. Appl. Phys. (pt.1), 1994. **33**: p. 2348-53.
35. Vescan, L., et al. *Properties of Si/SiGe quantum dots and wires growth by selective epitaxy*. in *1st international conference on Materials for Microelectronics*. 1995. Barcelona, Spain: Mat. Sci. Tech.
36. Tang, Y.S., et al., *Elastic strain and enhanced light emission in dry etched Si/SiGe quantum dots*. J. Electron. Lett., 1996. **25**(2): p. 287-91.
37. Tang, Y.S., et al. *Optical properties of Si-SiGe quantum dots and antidots*. in *International Conference on the Physics of Semiconductors*. 1996. Berlin: World Scientific.
38. J.L.Liu, W.G. Wu, A. Balandin, G.L. Jin, K.L. Wang, *Intersubband absorption in boron-doped multiple Ge quantum dot*, Applied Physics Letters, **74**, 185 (1999).
39. Liu, J.L.; Wu, W.G.; Balandin, A.; Jin, G.; Luo, Y.H.; Thomas, S.G.; Lu, Y.; Wang, K.L. *Observation of inter-sub-level transitions in modulation-doped Ge quantum dot*. Applied Physics Letters, **75**, AIP, 20 (1999), p.1745-7.
40. Konkar, A., A. Madhukar, and P. Chen, *Stress-engineered spatially selective self-assembly of strained InAs quantum dots on non-planar patterned (001) GaAs substrates*. Appl. Phys. Lett., 1998. **72**(2): p. 220-2.
41. Zhu, J.H., K. Brunner, and G. Abstreiter, *Two-dimensional ordering of self-assembled Ge islands on vicinal Si (001) surfaces with regular ripples*. Appl. Phys. Lett., 1998. **73**(5): p. 620-2.
42. DeWolf, I., et al., *Micro-Raman study of stress distribution in local isolation structures and correlation with transmission electron microscopy*. J. Appl. Phys., 1992. **71**(2): p. 898-906.

UCLA Equipment Management Department - Final Equipment Inventory Report - Report Date: August 9, 2000

Agency	ARMY	Fund	23040
Award Number	DAAH04-96-1-0364	Principal Investigator	KANG L. WANG

ORDER NO.	UCLA NO.	GOV'T. I.D.	DESCRIPTION	MFGR. NAME	MODEL NO.	SERIAL NO.	VALUE	CP/GFE	COMMENTS
<i>Items To Which The University Has Title:</i>									
0P7A058	964012187		COMPUTER, KSA 400, COMPLETE SYSTEM	K-SPACE	KSA-400	N/A	\$14,508.00	CP	
0P7A118	974002792		SI-MBE SYSTEM	BLT	GS6	N/A	\$263,850.00	CP	SPLIT FUNDED: 23040 & 51561; UC INV. \$346,132.50
0P8D595	984000593		COMPACT MODULAR PLASMA SYSTEM	PLASMALAB	80 PLUS	N/A	\$26,093.00	CP	SPLIT FUNDED: 22984, 23040 & 53890; UC \$125,570.00

Number of Items	3	Subtotal - Agency	\$0.00
		Subtotal - University	\$304,451.00